METROLOGY AND MEASUREMENT SYSTEMS
VOL. XIV, NUMBER 3 (2007)

MACIEJ WAWRZYNIAK

Poznań University of Technology
Faculty of Electronics and Telecommunications
Poland, e-mail: mwawrz@et.put.poznan.pl

PROBE CAPACITANCE-DEPENDENT SYSTEMATIC ERROR IN I-V MEASUREMENTS OF NANOWIRES: ANALYSIS AND CORRECTION

We propose a method of eliminating the systematic error due to the capacitance of digital oscilloscope probes in the experimental setup used for tracing current-voltage (I-V) curves of nanowires with quantum point contact (QPC). Used in I-V measurements, a digital storage oscilloscope (DSO) allows a reduction of measurement time to microseconds. Such short measurement time, however, involves a sensible effect of transition states occurring in an experimental setup representing an RC circuit. We analyze the effect of probe capacitance on the signal reading and on the resulting I-V curves, and derive theoretical formulae for the probe capacitance-dependent systematic error on the basis of a model proposed for the discussed measurement method. The systematic error is evidenced by nonlinearity of the obtained current-voltage curve, its shift with respect to the origin of the coordinate system, and an extension of the measurement range. We propose a correction method based on the derived theoretical relations that allow to calculate the corrections to be applied. The presented results of I-V measurements of nanowires with QPC confirm the correctness of our model and the effectiveness of the method proposed.

Keywords: nanotechnology, nanowires, quantum point contacts, conductance quantization, conductance measurements, current-voltage curves

1. INTRODUCTION

Electron transport in nanowires has recently become the subject of increasing scientific interest. As the continuous progress in electronic circuit integration involves the necessity of using components of nanometer dimensions, nanowires have already found application in diodes [1, 2], field-effect transistors [3, 4] and single electron tunneling transistors [5]. Nanowires used in these devices have diameter of tens to hundreds nanometers. This paper discusses a method of nanowire fabrication and I-V measurements that allows investigation of electric properties of nanowires with QPC of single atom diameter.

Nanowires were first found to be formed by means of a scanning tunneling microscope (STM) in an experiment by Gimzewski and Möller [6] in 1987. Conductance quantization was first observed in 1993, in gold nanowires with QPC fabricated by

means of an STM at room temperature and atmospheric pressure [7, 8]. Further studies lead to the development of other methods of fabricating nanowires with QPC, requiring a setup much less sophisticated than an STM, as nanowires were found to be formed also between two macroscopic wires [9] (1995) or between relay contacts [10, 11] (1997). The effect of spontaneous formation of nanowires with QPC between macroscopic metallic electrodes [12, 13] is used in the experimental investigation of nanowire properties. Two electrodes are brought to collision, after which one of them is retracted at an appropriate speed which results in nanowire formation between the electrodes. The nanowires are drawn until they break, and the last one to remain between the electrodes just before breaking forms a QPC in its narrowest point. Measurements of the conductance of such a nanowire as a function of time will yield a plot like that shown in Fig. 1, with steps due to the effect of conductance quantization. The nanowire conductance takes on quantized values: ..., $4G_0$, $3G_0$, $2G_0$, $1G_0$, where G_0 is determined by the following relation:

$$G_0 = \frac{2e^2}{h}, \tag{1}$$

e denoting the elementary charge and h being Planck's constant.

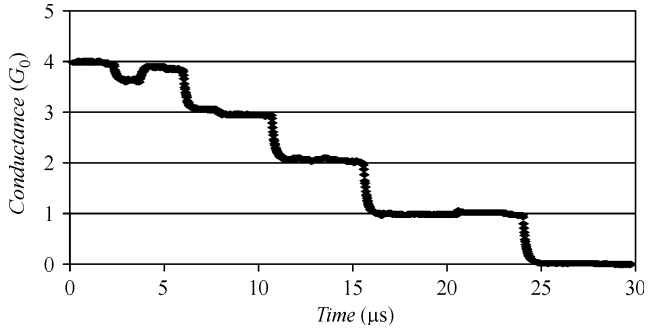

Fig. 1. Results of conductance measurements performed in a gold nanowire during its drawing, plotted versus time.

Figure 1 shows the ideal case where the electron transport within the nanowire is ballistic (no scattering occurs). When electrons are subject to scattering in the nanowire, extra conductance plateaus appear between values kG_0. (k = 1, 2, ...). The method of nanowire fabrication between macroscopic electrodes has been used for studying conductance quantization in metals [14, 15], metal alloys [16, 17], and metallic oxide crystals [18]. In an enhanced version of this method the STM mechanism is used for electrode driving [19, 20]. The STM-based method of mechanical production of nanowires has also been used for I-V measurements of nanowires with QPC [14, 19–21]. Nanowires drawn in this way are not stable, though. Each stepwise change in the conductance plot depicted in Fig. 1 involves atom rearrangement in the nanowire;

the plateaus at levels kG_0 (k = 1, 2, ...) correspond to successive metastable atom configurations. The time of I-V measurements must not go beyond the duration of the current atom configuration; in the case of the discussed nanowire, this implies measurement time limits 7.6 μs, 3.9 μs, and 4 μs for conductance values $1G_0$, $2G_0$, and $3G_0$, respectively. Inversely proportional to the speed at which the nanowire is drawn, the duration of the conductance plateaus imposes time requirements to be met by the experimental setup used for I-V measurements [19, 20]. The short measurement time involves an impact of transition states occurring in the setup circuit, and consequently, a systematic error in the measurements. This can be revealed, among others, by the current-voltage curve not passing through the origin of the coordinate system [22], or by the occurrence of a physically inexplicable nonlinearity. The right interpretation of the measurement data requires elimination of the systematic error through the application of a suitable correction procedure.

2. SETUP

Figure 2 shows a modified block diagram of an experimental setup for I-V measurements proposed by Hansen *et al.* [20]. Nanowires are formed between the electrodes labeled A and B. The tip-shaped electrode A is fixed to the head of a piezoelectric actuator (PI P250.20 HVPZT). The motion of the actuator head is controlled by an Agilent 33220A function generator (labeled 1) and the generated voltage signal is amplified by a high-voltage amplifier (PI E-461). The function generator 1 is controlled from a PC through a GPIB interface, which allows proper setup of the range and speed of the motion of electrode B. Measurements are initiated by triggering generator 1. The generated control signal is applied to the piezoelectric actuator, bringing electrodes A and B to collision and then retracting electrode B from electrode A. The nanowires produced during this retraction are drawn to break in turns, until a single one remains, forming a QPC just before breaking. Applied to the nanowire produced in this way, voltage V_{DC} from the DC power supply unit (Agilent E3631) results in the generation of current i_Q. The current signal is converted by the I/V converter into a voltage signal v_1, entering through channel 1 the digital storage oscilloscope (DSO) where it is measured.

Before measurements the oscilloscope trigger level must be set up at the value corresponding to the conductance level kG_0. (k = 1, 2, ...) at which the current-voltage curve is to be determined. Upon triggering the oscilloscope generates the external TTL *TrigOut* signal which is used to trigger the function generator 2 (Agilent 33220A). Added to V_{DC}, function generator 2 output signal, v_{FG}, alters the current i_Q in the nanowire throughout the I-V measurement range.

Figure 3 shows the equivalent diagram of the measurement circuit, with R_Q representing the resistance of the nanowire and R_P the internal resistance of the I/V converter. Signal $v_2(t)$, or the sum of the DC supply signal V_{DC} and the function ge-

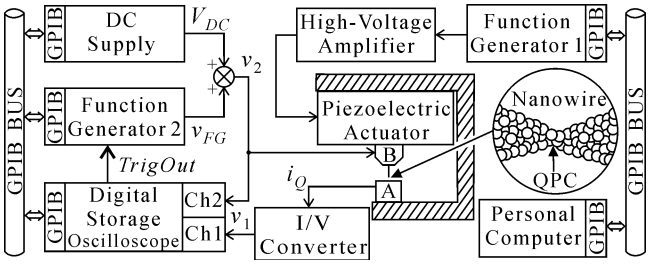

Fig. 2. Block diagram of the experimental setup.

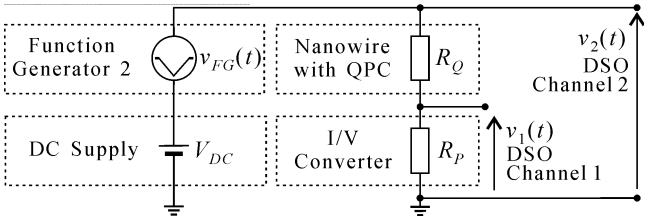

Fig. 3. Equivalent diagram of the measurement circuit.

nerator signal $v_{FG}(t)$, enters the oscilloscope through channel 2. Channel 1 is reserved for the incoming I/V converter output signal $v_1(t)$. Through the sampling process, the analog signals $v_1(t)$ and $v_2(t)$ are converted to discrete ones, which can be expressed as follows:

$$v'_n = v_1(nT_S) \quad \text{for} \quad n = 0, 1, 2, ..., N-1, \tag{2}$$

$$v''_n = v_2(nT_S) \quad \text{for} \quad n = 0, 1, 2, ..., N-1, \tag{3}$$

N being the number of samples taken and T_S denoting the sampling period; $v_1(nT_S)$ and $v_2(nT_S)$ are the values of voltage signals $v_1(t)$ and $v_2(t)$, respectively, in samples taken at moment nT_S. Another operation performed by the digital oscilloscope is signal quantization by using a finite number of codes for measurement of each voltage sample. This results in a digital signal. The voltage levels assigned to signals v_1 and v_2 can be found from the following relation:

$$v_1(nT_S) = \left(y_1(nT_S) - y_{ref1}\right) y_{inc1} + y_{org1}, \tag{4}$$

$$v_2(nT_S) = \left(y_2(nT_S) - y_{ref2}\right) y_{inc2} + y_{org2}, \tag{5}$$

where $y_1(nT_S)$ and $y_2(nT_S)$ are the codes obtained through A/D conversion of a sample taken at moment nT_S (channel 1 and 2, respectively); y_{ref1}, y_{inc1}, y_{org1} and y_{ref2}, y_{inc2}, y_{org2} are scaling coefficients dependent on the amplification coefficient setup in

the respective channels. Including (4) in (2) and (5) in (3) results in the following formulae for the digital signal reading, v'_n and v''_n, obtained from analog signals $v_1(t)$ and $v_2(t)$:

$$v'_n = \left(y_1(nT_S) - y_{ref1}\right) y_{inc1} + y_{org1} \quad \text{for} \quad n = 0, 1, 2, \ldots, N-1, \tag{6}$$

$$v''_n = \left(y_2(nT_S) - y_{ref2}\right) y_{inc2} + y_{org2} \quad \text{for} \quad n = 0, 1, 2, \ldots, N-1. \tag{7}$$

Transferred through the GPIB interface to the PC, the signal reading is stored in a file. As can be deduced from the diagram shown in Fig. 3, the nanowire voltage values at the moment of sampling can be found from the following relation:

$$v_n = v''_n - v'_n \quad \text{for} \quad n = 0, 1, 2, ..., N-1. \tag{8}$$

The current in the nanowire at the moment of sampling can be calculated from:

$$i_n = \frac{v'_n}{R_P} \quad \text{for} \quad n = 0, 1, 2, ..., N-1. \tag{9}$$

The current-voltage curve of the nanowire is traced by plotting the values (v_n, i_n) ($n = 0, 1, 2, ..., N-1$) in the xy coordinate system. The number of points in the plot will be equal to that of signal samples taken.

3. EXPERIMENTAL

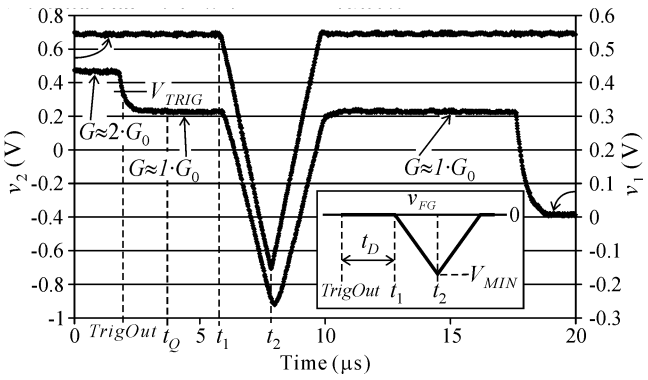

Fig. 4. Measured values of voltage signals $v_1(t)$ and $v_2(t)$.

Figure 4 shows the values of signals v_1 and v_2 acquired through I-V measurements of a gold nanowire drawn at 16 μm/s speed. The measurements were performed at room temperature and atmospheric pressure. The setup was configured for I-V measurements

at conductance value $G = 1G_0$, which involves oscilloscope triggering at the moment of the stepwise decrease in nanowire conductance from $G = 2G_0$ to $G = 1G_0$. As can be deduced from the diagram depicted in Fig. 3, the value of v_1 before triggering of the function generator 2 is determined by the following relation:

$$v_1 = V_{DC}\frac{R_P}{R_Q + R_P}, \tag{10}$$

where $R_P = 10.04$ kΩ is the internal resistance of the I/V converter, $V_{DC} = 0.700$ V is the DC supply voltage, $R_Q \approx 6.45$ kΩ for $G = 2G_0$, and $R_Q \approx 12.9$ kΩ for $G = 1G_0$. The v_1 values found from this relation are 0.426 V for $G = 2G_0$ and 0.306 V for $G = 1G_0$. The intermediate voltage value $V_{TRIG} = 0.366$ V was assumed as the trigger level. The other trigger settings were as follows: trigger source: channel 1, trigger coupling: DC, trigger type: edge, trigger slope: falling. Such settings ensure the oscilloscope will be triggered at the moment of the stepwise decrease in conductance value from $G = 2G_0$ to $G = 1G_0$. The *TrigOut* signal generated by the oscilloscope triggers the function generator 2, which generates output signal v_{FG} that is added to V_{DC}. Plotted versus time, signal v_{FG} is shown in Fig. 4 (inset), showing also the time delay, t_D, followed by the time interval from t_1 to t_2 in which the signal is used for I-V measurements. It is the data corresponding to that time interval that is used for building the current-voltage curve. Both the delay t_D and the time interval $t_2 - t_1$ must be adapted to the speed of nanowire drawing (*i.e.* that of electrode B retracting from electrode A). In the measurements which yielded the data depicted in Fig. 4, the function generator 2 was programmed so as to obtain a time interval $t_2 - t_1 = 2\mu$s. Determining the I-V measurement range, V_{MIN}, the amplitude of signal v_{FG}, was set at $V_{MIN} = -2V_{DC}$, allowing measurements in the range:

$$\left\langle -V_{DC}\frac{R_Q}{R_Q + R_P}, V_{DC}\frac{R_Q}{R_Q + R_P}\right\rangle. \tag{11}$$

With moment t_1 assumed as the reference time ($t_1 = 0$), the following relation is fulfilled by the time-dependent signal from function generator 2 in the time interval from t_1 do t_2:

$$v_{FG} = Wt, \tag{12}$$

where W, denoting the rate of v_{FG} change, can be found from:

$$W = \frac{V_{MIN}}{t_2 - t_1}; \tag{13}$$

V_{MIN} (the minimum voltage value) and $t_2 - t_1$ (voltage decrease time) are parameters of signal v_{FG} determined by the settings of function generator 2. The values of V_{DC} and W are calculated from data acquired for signal v_2 in the time interval from t_1 to

t_2. By assuming $t_1 = 0$, applying (7) to express the digital signal sample values, and using linear regression, W and V_{DC} can be expressed by the following formulae:

$$W = \frac{\sum_{n=0}^{N-1}(nT_S v_n'') - \frac{1}{N}\sum_{n=0}^{N-1}(nT_S)\sum_{n=0}^{N-1} v_n''}{\sum_{n=0}^{N-1}(nT_S)^2 - \frac{1}{N}\left(\sum_{n=0}^{N-1}(nT_S)\right)^2}, \tag{14}$$

$$V_{DC} = \frac{\sum_{n=0}^{N-1} v_n'' - W\sum_{n=0}^{N-1}(nT_S)}{N}, \tag{15}$$

where N is the number of samples taken in the time interval from t_1 to t_2.

Calculated on the basis of (14) and (15), the values for the parameters in question are: $W = (-700 \pm 4)10^3$ V/s and $V_{DC} = (0.700 \pm 0.004)$ V.

The resistance, R_Q, of the nanowire with QPC was determined on the basis of the values of $v_1(t)$ in the time interval from t_Q to t_1, from the following formula, obtained by assuming $t_Q = 0$ and using (6) to express the digital signal sample values:

$$R_Q = R_P\left(\frac{V_{DC}}{\frac{1}{N}\sum_{n=0}^{N-1} v_n'} - 1\right), \tag{16}$$

where N is the number of samples taken in the time interval from t_Q to t_1.

Calculated on the basis of (16), the value of resistance R_Q for the signal $v_1(t)$ shown in Fig. 4 is $R_Q = 12.75$ kΩ (1.012 G_0). Once the generated signal v_{FG} vanishes, voltage v_1 recovers the value it had before the activation of function generator 2. This means the conductance of the nanowire has not changed in the time of tracing signals $v_1(t)$ and $v_2(t)$ and the acquired data can be used for tracing the current-voltage curve. Once the $v_1(t)$ and $v_2(t)$ values depicted in Fig. 4 have been acquired, the data corresponding to the time interval from t_1 to t_2 is computer-processed and used for constructing the I-V chart on the basis of (8) and (9).

Figure 9 shows the current-voltage curve (the diamonds) traced on the basis of the measurement data presented in Fig. 4. The obtained curve does not pass through the origin of the coordinate system: a nonzero current value corresponds to voltage $V = 0$. Also, the characteristic shows nonlinearity in its part corresponding to $V > 0.25$ V. This is due to the capacitance of the passive probes used for measuring signals $v_1(t)$ and $v_2(t)$.

4. THEORETICAL ANALYSIS OF THE EFFECT OF PROBE CAPACITANCE

Figure 5a shows the equivalent diagram of a high-impedance passive probe with magnification factor 10:1 (X10), connected to an oscilloscope. In the diagram shown in Fig. 5a resistor R_2 and capacitor C_{OS} represent the oscilloscope input resistance and its input capacitance, respectively. The values of these parameters in the oscilloscope used in the experimental setup in question are R_2 = 1 MΩ and C_{OS} = 15 pF. Resistors R_1 and R_2 act as a voltage divider. The R_1 value corresponding to a X10 probe is 9 MΩ. The probe input resistance results from that of resistors R_1 and R_2 connected in series. The controllable capacitor C_{COMP} is used for probe compensation. Capacitor C_{CC} represents the capacitance of the coaxial cable with respect to ground; its values range from 25 pF/m to 50 pF/m, depending on the cable type. Resistor R_{CC} represents the resistance of the coaxial cable core. Resistor R_1 and capacitor C_H are situated in the probe tip casing at the side of the measured signal. Connected in series with the capacitance sum $C_{CC} + C_{COMP} + C_{OS}$, capacitor C_H reduces the input capacitance of the probe connected to the oscilloscope. The diagram does not show resistors (of resistance values in the order of tens to hundreds ohms) placed inside the probe for eliminating signal reflection.

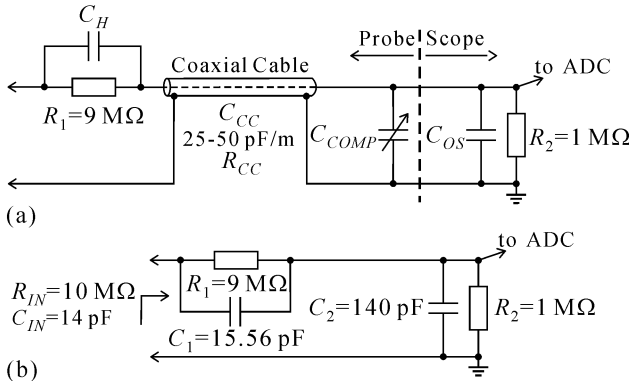

Fig. 5. The equivalent diagram of a high-impedance passive probe (a); the model of the probe connected to the oscilloscope, used in this analysis (b).

Our analysis is based on the simplified equivalent diagram shown in Fig. 5b, of a probe connected to the oscilloscope. Probe manufacturers tend to specify the input resistance, R_{IN}, and the input capacitance, C_{IN}, of the probe connected to an oscilloscope and compensated. In the probes applied in our setup the values of these parameters were C_{IN} = 14 pF and R_{IN} = 10 MΩ. The resistance of the coaxial cable core and that of the resistors eliminating signal reflection can be neglected. Probes must be compensated before use, following the relevant instructions included in the oscilloscope user's guide. Once the probe is compensated, the following condition is fulfilled in the equivalent diagram shown in Fig. 5b:

$$R_1 C_1 = R_2 C_2. \tag{17}$$

The circuit also satisfies the equation:

$$\frac{1}{C_{IN}} = \frac{1}{C_1} + \frac{1}{C_2}. \tag{18}$$

By transforming (17) and (18) and putting the respective resistance values in place of R_1 and R_2, the following formulae are obtained, allowing to find the capacitance values of capacitors C_1 and C_2 in the equivalent diagram:

$$C_1 = \frac{10}{9} C_{IN}, \tag{19}$$

$$C_2 = 9C_1. \tag{20}$$

The calculated values are $C_1 = 15.56$ pF and $C_2 = 140$ pF. The diagram in Fig. 6 represents the circuit used for measuring signals $v_1(t)$ and $v_2(t)$, taking into account the capacitance and resistance of the oscilloscope probes, as well as the input capacitance and resistance of the oscilloscope channels 1 and 2. Capacitors $C_1 = 15.56$ pF and $C_2 = 140$ pF, and resistors $R_1 = 9$ MΩ and $R_2 = 1$ MΩ represent a probe connected to the oscilloscope through its channel 1. Capacitors $C_3 = 15.56$ pF and $C_4 = 140$ pF, and resistors $R_3 = 9$ MΩ and $R_4 = 1$ MΩ represent the probe connected to the oscilloscope through its channel 2. Resistor $R_P = 10.04$ kΩ represents the internal resistance of the I/V converter, and $R_Q = 12.75$ kΩ is the nanowire resistance at conductance level $G = 1.012\ G_0$. Switch Sw_1 is opened at moment $t = 0$, which is the moment of triggering function generator 2. From that moment on, signal v_{FG} from the function generator is added to signal V_{DC}, producing transition states in the circuit.

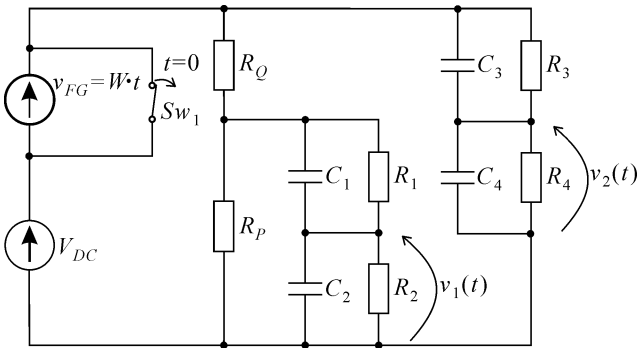

Fig. 6. The diagram of the circuit used for measuring signals $v_1(t)$ and $v_2(t)$, taking into account the capacitance and resistance of the oscilloscope and the oscilloscope probes.

Formulae describing v_1 and v_2 as functions of time for $t \geq 0$ were derived on the basis of the diagram shown in Fig. 6. The subscript *RC* indicates the oscilloscope probe capacitance and resistance have been taken into account in the derivation. Thus, the value of voltage $v_{2RC}(t)$ can be found from:

$$v_{2RC}(t) = B_1 + B_2 t + B_3 e^{B_4 t}, \tag{21}$$

where constants B_1, B_2, B_3, B_4 can be determined from the respective formulae compiled in Table 1.

Table 1. Formulae for the constants in (21) and (22).

Constant	Formula
B_1	$\frac{A_2}{A_4} - \frac{A_3}{A_4^2}$
B_2	$\frac{A_3}{A_4}$
B_3	$A_1 - \frac{A_2}{A_4} + \frac{A_3}{A_4^2}$
B_4	$-A_4$
A_1	$\frac{V_{DC} R_4}{R_3 + R_4}$
A_2	$\frac{V_{DC} + W R_3 C_3}{R_3 (C_3 + C_4)}$
A_3	$\frac{W}{R_3 (C_3 + C_4)}$
A_4	$\frac{R_3 + R_4}{(R_3 R_4)(C_3 + C_4)}$
B_5	$\frac{A_7 A_{11} - A_8 A_{10}}{A_{11}^2}$
B_6	$\frac{A_8}{A_{11}}$
B_7	$\frac{-A_{10} + \sqrt{A_{10}^2 - 4 A_9 A_{11}}}{2 A_9}$
B_8	$\frac{-A_{10} - \sqrt{A_{10}^2 - 4 A_9 A_{11}}}{2 A_9}$
B_9	$\frac{A_5 A_{11}^2 B_7 + B_7 A_9 (A_8 A_{10} - A_7 A_{11}) + A_{11} (A_6 A_{11} - A_7 A_{10}) + A_8 \left(A_{10}^2 - A_9 A_{11}\right)}{A_{11}^2 A_9 (B_7 - B_8)}$

B_{10}	$\dfrac{A_5A_{11}^2B_8 + B_8A_9\left(A_8A_{10} - A_7A_{11}\right) + A_{11}\left(A_6A_{11} - A_7A_{10}\right) + A_8\left(A_{10}^2 - A_9A_{11}\right)}{A_{11}^2A_9\left(B_8 - B_7\right)}$
A_5	$\dfrac{V_{DC}R_pR_2C_1C_2}{R_Q\left(R_1 + R_2 + R_p\right) + R_p\left(R_1 + R_2\right)}$
A_6	$V_{DC}R_p\dfrac{\left(\dfrac{1}{R_Q} + \dfrac{1}{R_p} + \dfrac{1}{R_1}\right)\left(R_2C_2 - R_1C_1\right) + C_1}{R_Q\left(\left(R_1 + R_2 + R_p\right) + R_p\left(R_1 + R_2\right)\right)} + \dfrac{C_1V_{DC}}{R_Q}$
A_7	$\dfrac{V_{DC} + WC_1R_1}{R_1R_Q}$
A_8	$\dfrac{W}{R_QR_1}$
A_9	C_1C_2
A_{10}	$\left(\dfrac{1}{R_Q} + \dfrac{1}{R_p} + \dfrac{1}{R_1}\right)\left(C_1 + C_2\right) + \left(\dfrac{1}{R_1} + \dfrac{1}{R_2}\right)C_1 - \dfrac{2C_1}{R_1}$
A_{11}	$\left(\dfrac{1}{R_Q} + \dfrac{1}{R_p} + \dfrac{1}{R_1}\right)\left(\dfrac{1}{R_1} + \dfrac{1}{R_2}\right) - \dfrac{1}{R_1^2}$

The similar formula for voltage $v_{1RC}(t)$ reads:

$$v_{1RC}\left(t\right) = B_5 + B_6t + B_9e^{B_7t} + B_{10}e^{B_8t}, \tag{22}$$

the formulae for constants B_5, B_6, B_7, B_8, B_9 and B_{10} being provided in Table 1.

The oscilloscope probe input capacitance values were assumed to be negligible in the ideal case. Formulae for v_1 and v_2 as functions of time were derived, for $t \geq 0$, on the basis of the diagram shown in Fig. 6 without capacitors C_1, C_2, C_3, C_4. The subscript R indicates the probe resistance only has been taken into account in the derivation of the formulae for $v_{2R}(t)$ and $v_{1R}(t)$:

$$v_{2R} = \left(V_{DC} + Wt\right)\frac{R_4}{R_3 + R_4}, \tag{23}$$

$$v_{1R} = \left(V_{DC} + Wt\right)\frac{R_PR_2}{R_Q\left(R_1 + R_2 + R_P\right) + R_P\left(R_1 + R_2\right)}. \tag{24}$$

The theoretical voltage values v_{1R} calculated on the basis of (24) (the model not taking into account the probe capacitance), the theoretical voltage values v_{1RC} calculated on the basis of (22) (the model taking into account the probe capacitance), and the v_1 values found experimentally (see Fig. 4) in the time interval from $t_1 = 0$ μs to $t_2 = 2$ μs are compared in the superimposed plots shown in Fig. 7a.

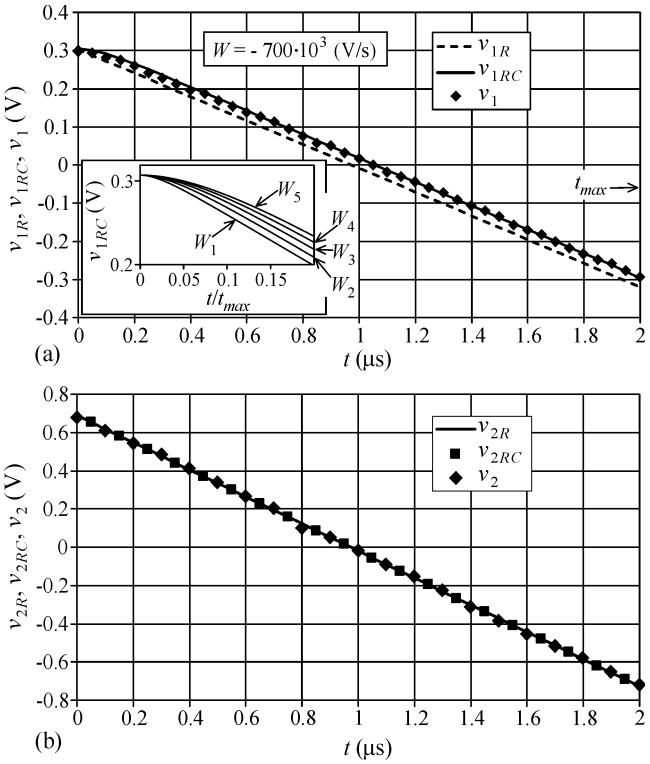

Fig. 7. Superimposed plots representing theoretical and experimental data: (a) v_{1R} and v_{1RC} represent theoretical voltage values calculated on the basis of the model without and with probe capacitance taken into account, respectively; v_1 are the corresponding experimental data; (b) v_{2R} and v_{2RC} represent theoretical voltage values calculated on the basis of the model without and with probe capacitance taken into account, respectively; v_2 are the corresponding experimental data. Inset in (a): $v_{1RC}(t)$ for different values of $W(W_1 = -0.4 \cdot 10^6$ V/s, $W_2 = -0.7 \cdot 10^6$ V/s, $W_3 = -1.0 \cdot 10^6$ V/s, $W_4 = -1.3 \cdot 10^6$ V/s, $W_5 = -1.6 \cdot 10^6$ V/s).

Similarly, Fig. 7b shows superimposed plots of v_{2R} (theoretical values calculated from (23) on the basis of the model not taking into account the probe capacitance), v_{2RC} (theoretical values calculated from (21) on the basis of the model that does take into account the probe capacitance) and v_2 (experimental data from the time interval $t_1 = 0$ μs to $t_2 = 2$ μs, see Fig. 4). The experimental data used in the plot involve the assumption $t_1 = 0$ and the consequent shift along the time axis. A portion of the $v_1(t)$ and $v_2(t)$ data is omitted for clarity reasons. The theoretically calculated values of parameters W and V_{DC} are: $W = -700\ 10^3$ V/s and $V_{DC} = 0.700$ V. The results of calculations based on the theoretical formulae must be multiplied by 10, as the probes used in the experimental setup divide the measured signals with ratio 10:1. In digital oscilloscopes a voltage divider probe either is detected automatically or requires an appropriate user configuration. In each case the oscilloscope reading is multiplied by

10, yielding actual sample values of the voltage signals at the oscilloscope input. The presented plots reveal a systematic error, due to the effect of the probe capacitance, of the measured signals $v_1(t)$ and $v_2(t)$. Figures 7a and 7b indicate the error is more significant in the case of signal $v_1(t)$. Superimposed in Fig. 7a, the plots of $v_{1RC}(t)$ and $v_1(t)$ coincide, proving the correctness of the assumed model of the probes and the experimental setup (Fig. 6), but are shifted with respect to the $v_{1R}(t)$ plot, and show nonlinearity, which is especially in evidence in the time interval just after opening switch Sw_1 (see Fig. 6), *i.e.* immediately after activating function generator 2, which generates signal v_{FG}.

The plots in Fig. 7a correspond to $W = -700\ 10^3$ V/s. Plots of $v_{1RC}(t)$ corresponding to different values of W ($W_1 = -0.4\ 10^6$ V/s, $W_2 = -0.7\ 10^6$ V/s, $W_3 = -1.0\ 10^6$ V/s, $W_4 = -1.3\ 10^6$ V/s, $W_5 = -1.6\ 10^6$ V/s) are compared in Fig. 7a inset. The systematic error increases with increasing v_{FG} rate of change (absolute value). The theoretical value of the time-dependent systematic error (absolute and relative) can be determined from the following formulae:

$$\Delta_1(t) = v_{1RC}(t) - v_{1R}(t), \tag{25}$$

$$\delta_1 = \frac{v_{1RC} - v_{1R}}{v_{1R}}. \tag{26}$$

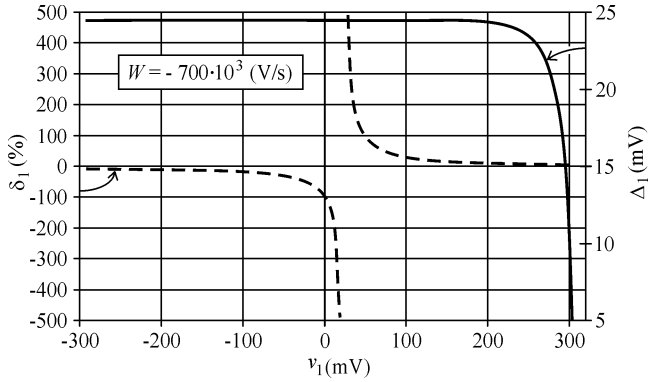

Fig. 8. Theoretical values of absolute systematic error Δ_1 (solid line) and relative systematic error δ_1 (dashed line) in the measured signal v_1 at $W = -700 \cdot 10^3$ V/s.

Figure 8 shows errors Δ_1 and δ_1 calculated from (25) and (26) plotted versus the measured value of v_1 for $W = -700\ 10^3$ V/s.

5. CORRECTION OF THE SYSTEMATIC ERROR

Current-voltage characteristics are traced on the basis of measurements of signals $v_1(t)$ and $v_2(t)$ in the time interval from t_1 to t_2 (Fig. 4). Signals $v_1(t)$ and $v_2(t)$ in the experimental setup are measured over a period of time longer than the interval from t_1 to t_2; the data corresponding to that time interval is to be set apart, which implies a shift of the reference time. The digital oscilloscope performs signal sampling and quantization, converting the input analog signals into digital ones, expressed by (6) and (7). Let us assume $t_1 = 0$ and express the moments of digital signal sampling as:

$$t_n = n \cdot T_S \quad \text{for} \quad n = 0, 1, 2, \ldots, N. \tag{27}$$

We propose the following two-step correction procedure in order to eliminate the probe capacitance-dependent systematic error in I-V measurements. In the first step, corrections to be applied to individual signal $v_1(t)$ and $v_2(t)$ samples taken at moments t_n are determined from the following formulae:

$$p'_n = -\left(v_{1RC}\left(t_n\right) - v_{1R}\left(t_n\right)\right) \quad \text{for} \quad n = 0, 1, 2, \ldots, N-1, \tag{28}$$

$$p''_n = -\left(v_{2RC}\left(t_n\right) - v_{2R}\left(t_n\right)\right) \quad \text{for} \quad n = 0, 1, 2, \ldots, N-1, \tag{29}$$

where p'_n and p''_n denote the corrections to signals $v_1(t)$ and $v_2(t)$, respectively; $v_{1RC}(t_n)$, $v_{1R}(t_n)$, $v_{2RC}(t_n)$, $v_{2R}(t_n)$ and t_n are calculated from the respective formulae (22), (24), (21), (23) and (27).

In the next step, the points of the current-voltage curve are calculated from the following equations:

$$v_n = \left(v''_n + p''_n\right) - \left(v'_n + p'_n\right) \quad \text{for} \quad n = 0, 1, 2, \ldots, N-1, \tag{30}$$

$$i_n = \frac{v'_n + p'_n}{R_p} \quad \text{for} \quad n = 0, 1, 2, \ldots, N-1. \tag{31}$$

In order to compare the resulting characteristic with the theoretical curves determined through calculations on the basis of the two models discussed, without and with the effect of probe capacitance taken into account, I-V points were calculated from the theoretical formulae derived for the ideal case, without the effect of probe capacitance:

$$v_n = v_{2R}\left(t_n\right) - v_{1R}\left(t_n\right) \quad \text{for} \quad n = 0, 1, 2, \ldots, N-1, \tag{32}$$

$$i_n = \frac{v_{1R}\left(t_n\right)}{R_p} \quad \text{for} \quad n = 0, 1, 2, \ldots, N-1, \tag{33}$$

and from those derived on the basis of the model that does take into account the effect of probe capacitance:

$$v_n = v_{2RC}(t_n) - v_{1RC}(t_n) \quad \text{for} \quad n = 0, 1, 2, \ldots, N-1, \tag{34}$$

$$i_n = \frac{v_{1RC}(t_n)}{R_p} \quad \text{for} \quad n = 0, 1, 2, \ldots, N-1. \tag{35}$$

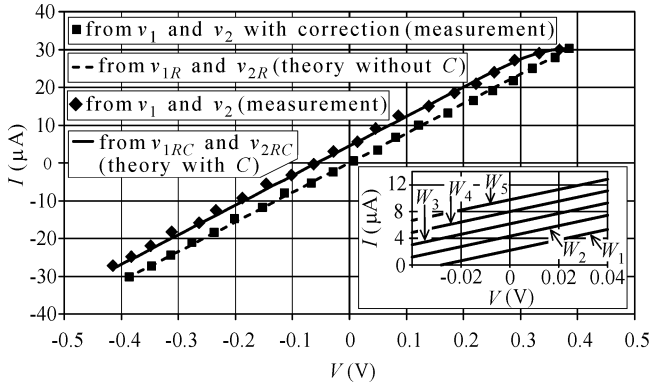

Fig. 9. The current-voltage curve traced on the basis of the data obtained through measurements of signals $v_1(t)$ and $v_2(t)$ shown in Fig. 4, without error correction (diamonds) and with error correction (squares), superimposed with the I-V curve found theoretically within the model without and with probe capacitance taking into account (dashed and solid line, respectively). Inset: current-voltage curves obtained through calculations assuming different values of W ($W_1 = -0.4\ 10^6$ V/s, $W_2 = -0.7\ 10^6$ V/s, $W_3 = -1.0\ 10^6$ V/s, $W_4 = -1.3\ 10^6$ V/s, $W_5 = -1.6\ 10^6$ V/s).

The resulting current-voltage curves are shown in Fig. 9. The current-voltage curve obtained from the measurement data (the diamonds in Fig. 9) coincides, with good approximation, with that found theoretically from the formula derived on the basis of the model taking into account the effect of probe capacitance (the solid line in Fig. 9). Opening the measurements, the point of coordinates $V = 0.392$ V and $I = 30.7$ μA coincides with its counterpart on the current-voltage curve found theoretically from the formula derived on the basis of the model without probe capacitance taken into account (the dashed line in Fig. 9). In the I-V characteristic obtained from measurement data the measurement range is extended appropriately. The x coordinate of the last measurement point is $V = -0.417$ V, against the value $V = -0.392$ V in the theoretical curve obtained on the basis of the model without probe capacitance taken into account. Also, the characteristic based on the experimental data shows nonlinearity, which is especially in evidence in that part of the current-voltage curve which represents the beginning of measurements (voltage values $V = 0.392$ V and below), *i.e.* measurements performed just after activation of function generator 2. A shift along the y axis is apparent, too:

at $V = 0$ V its value is $I = 4.131$ μA. The current-voltage curve shift along the y axis is a function of parameter W. The inset in Fig. 9 shows current-voltage curves obtained through calculations assuming different values of W ($W_1 = -0.4\ 10^6$ V/s, $W_2 = -0.7\ 10^6$ V/s, $W_3 = -1.0\ 10^6$ V/s, $W_4 = -1.3\ 10^6$ V/s, $W_5 = -1.6\ 10^6$ V/s) and performed on the basis of the model taking into account the effect of probe capacitance. Figure 9 shows also the I-V characteristic based on the measurement data to which the procedure of systematic error correction has been applied (the points of that curve are represented by squares). That curve coincides, with good approximation, with the 'ideal' one, obtained on the basis of the model without probe capacitance. This confirms the correctness of the model assumed as the basis of the theoretical formulae derived, and of the proposed correction procedure aimed at eliminating the systematic error due to the effect of the capacitance of the oscilloscope probes used in the measurements.

6. SUMMARY

We have shown how results of I-V measurements performed by means of a digital oscilloscope are affected by the oscilloscope probe capacitance, causing a systematic error. This error is found to occur in short-time I-V measurements (the measurement time being in the order of microseconds), in which the fast changes of the burst voltage applied to the studied nanowire involve the occurrence of transition states in the measurement circuit. The 10X passive probes used in the experimental setup have low input capacitance. Passive probes without a voltage divider (1X), having the input capacitance an order of magnitude higher, will produce an even larger systematic error in I-V measurements. The main results of this study include the derivation, on the basis of the model proposed, of theoretical formulae that allow to calculate the systematic error in voltage signal measurements aimed at tracing the I-V curve, as well as the proposed correction method eliminating the error and its effect on the I-V curves traced on the basis of the measurement data. In the proposed procedure, the corrections to be applied to the measurement data are determined on the basis of the theoretical formulae for the systematic error. The systematic error results in nonlinearity of the current-voltage curve, its shift with respect to the origin of the coordinate system, and an extension of the measurement range. Therefore, correction of the measurement data is necessary for proper interpretation of physical properties of the studied nanowires on the basis of their I-V charts. The measurement data and the calculation results presented in this study confirm the effectiveness of the correction method proposed.

ACKNOWLEDGEMENTS

This study is supported by the Polish Ministry of Science and Higher Education, grant N505 020 31/2968.

REFERENCES

1. Könenkamp R., Word R. C., Schlegel C.: *Vertical nanowire light-emitting diode*. Appl. Phys. Lett. vol. 85, no. 24, 2004, pp. 6004–6006.
2. Kim J.-R., Oh H., So H. M., Kim J., Kim J.-J.: *Rectifying diode made of individual gallium nitride nanowire*. Physica E, vol. 18, 2003, pp. 225–226.
3. Chang P.-C., Fan Z., Chien C.-J, Stichtenoth D., Ronning C., Lu J. G.: *High-performance ZnO nanowire field effect transistors*. Appl. Phys. Lett., vol. 89, 2006, pp. 133113–133115.
4. Zhou W. M., Fang F., Hou Z. Y., Yan L. J., Zhang Y. F.: *Field-Effect Transistor Based on β-SiC Nanowire*. IEEE Electron Device Letters, vol. 27, no. 9, 2006, pp. 463–465.
5. Hofheinz M., Jehl X., Sanquer M., Molas G., Vinet M., Deleonibus S.: *Simple and controlled single electron transistor based on doping modulation in silicon nanowires*. Appl. Phys. Lett., vol. 89, 2006, pp. 143504–143506.
6. Gimzewski J. K., Möller R.: *Transition from the tunneling regime to point contact tudied using scanning tunneling microscopy*. Phys. Rev. B, vol. 36, 1987, pp. 1284–1287.
7. Pascual J. I., Méndez J., Gómez-Herrero J., Baró A. M., García N.: *Quantum Contact in Gold Nanostructures by Scanning Tunneling Microscopy*. Phys. Rev. Lett., vol. 71, 1993, pp. 1852–1855.
8. Agrait N., Rodrigo J. G., Vieira S.: *Conductance steps and quantization in atomic-size contacts*. Phys. Rev. B, vol. 47, 1993, pp. 12345–12348.
9. Costa-Krämer J. L., García N., García-Mochales P., Serena P. A.: *Nanowire formation in macroscopic metallic contacts: quantum mechanical conductance tapping a table top*. Surface Science, vol. 342, 1995, pp. L1144–L1149.
10. Hansen K., Lagsgaard E., Stensgaard I., Besenbacher F.: *Quantized conductance in relays*. Phys. Rev. B, vol. 56, 1997, pp. 2208–2220.
11. Yasuda H., Sakai A.: *Conductance of atomic-scale gold contacts under high-bias voltages*. Phys. Rev. B, vol. 56, 1997, pp. 1069–1072.
12. Correia A., García N.: *Nanocontact and nanowire formation between macroscopic metallic contacts observed by scanning and transmission electron microscopy*. Phys. Rev. B, vol. 55, 1997, pp. 6689–6692.
13. Martinek J., Nawrocki W., Wawrzyniak M., Stankowski J.: *Quantized conductance of the nanowires spontaneously formed between macroscopic metallic contacts*. Molecular Physics Reports, vol. 20, 1997, pp. 157–163.
14. Costa-Krämer J. L., García N., García-Mochales P., Serena P. A., Marqués M. I., Correia A.: *Conductance quantization in nanowires formed between micro and macroscopic metallic electrodes*. Phys. Rev. B, vol. 55, 1997, pp. 5416–5424.
15. Kiguchi M., Konishi T., Murakoshi K.: *Hydrogen-assisted stabilization of Ni nanowires in solution*. Appl. Phys. Lett., vol. 87, 2005, pp. 43104–43106.
16. Enomoto A., Kurokawa S., Sakai A.: *Quantized conductance in Au-Pd and Au-Ag alloy nanocontacts*. Phys. Rev. B, vol. 65, pp. 125410–125415.
17. Enomoto A., Mizobata J.-I., Kurokawa S., Sakai A.: *Quantized conductance in AuAg nanocontacts under high biases*. Surface Science, vol. 514, 2002, pp. 182–186.
18. Ott F., Barberan S., Lunney J. G., Coey J. M. D., Berthet P., de Leon-Guevara A. M., Revcolevdchi A.: *Quantized conductance in a contact between metallic oxide crystals*. Phys. Rev. B, vol. 58, 1998, pp. 4656–4658.
19. Hansen K., Nielsen S. K., Bradbyge M., Lagsgaard E., Stensgaard I., Besenbacher F.: *Current-voltage curves of gold quantum point contacts revisited*. Appl. Phys. Lett., vol. 77, 2000, pp. 708–710.
20. Hansen K., Nielsen S. K., Lagsgaard E., Stensgaard I., Besenbacher F.: *Fast and accurate current-voltage curves of metallic quantum point contacts*. Rev. Sci. Instrum., vol 71, 2000, pp. 1793–1803.

21. Yoshida M., Oshima Y., Takayanagi K.: *Nonlinear current-voltage curves of gold quantum point contacts*. Appl. Phys. Lett., vol. 87, 2005, pp. 103104–103106.
22. Liu C. H., Yiu W. C., Au F. C. K., Ding J. X., Lee C. S., Lee S. T.: *Electrical properties of zinc oxide nanowires and intramolecular p – n junctions*. Appl. Phys. Lett., vol. 83, 2003, pp. 3168–3170.